

METHODOLOGICAL NOTES PACS number: 52.80.Tn

On physical processes in an 'open' discharge

P A Bokhan

DOI: https://doi.org/10.3367/UFNe.2018.04.038362

Contents

Abstract. This paper reviews the key features of the 'open' photoelectric discharge (FED) used for the high-efficiency generation of electron beams (EBs) in medium-pressure gases and for subnanosecond switching of high-voltage pulses. The energy efficiency of EB generation in both FEDs and anomalous discharges is measured, and conditions for the predominance of photoemission are formulated. It is concluded that the FED is a long-known phenomenon and that the arguments put forward in *Usp. Fiz. Nauk* 188 1354 (2018) [*Physics–Uspekhi* 61 1234 (12) (2018)] against its existence are based on simplified discharge models and poorly performed experiments and make use of other authors' results of no direct relevance to the 'open' discharge.

Keywords: open discharge, photoemission discharge, anomalous discharge, electron emission, electron beam generation, current–voltage characteristics

1. Introduction

The 'open' discharge (OD) term was coined by the authors of paper [1] for the gas discharge (GD) in short discharge gaps (DGs) between a continuous or grid cathode and an anode that must be without fail a grid anode, behind which there is an extended drift space (DS) bounded by an electron collector (EC). The OD concept is often extended to include other discharge types either not bounded by walls or restricted only partially. The OD, which is the subject of this publication, where the Dreicer criterion [2, 3] is significantly exceeded, $E/p \gg (E/p)_{cr}$, generates with high efficiency runaway electrons in the keV-energy range [4, 5] (E is the electric field strength, and p is the working-gas pressure). These electrons form an electron beam (EB) that carries energy away from the DG and causes luminescence of the working medium in the DS.

The first experiments [6, 7] have already shown that under certain conditions EB generation is greatly influenced by the additional photoillumination of the cathode from the DS, while gas ionization in the DG is unessential and is not the primary factor in OD development. Based on these observations, the authors of Ref. [8] introduced the term 'photoelectron discharge' (PED). The effect of an additional photoillumination was also confirmed in Ref. [1]. It was reflected in introducing the term 'open' discharge emphasizing the fact that the discharge characteristics are primarily affected by the discharge areas located outside the DG. However, the PED term was not used in Ref. [1], so the author of paper [9] incorrectly asserts his priority in introducing this term. Beginning with publication [10], he contests the decisive role of additional photo illumination from the DS and argues that the OD is a conventional anomalous discharge (AD). The goal of this publication is to draw some intermediate conclusions in studying OD properties and the physical processes that occur in that discharge as a response to publication [9].

2. Two 'simplest and apparent' arguments 'giving evidence that the photoemission discharge is a fiction'

The OD has been designed and implemented specifically to excite gas lasers [11]. It is for this reason that a coaxial electrode configuration has been used in the majority of studies involving the OD. The transverse size (diameter) of the cell, pressure p, and geometric transparency μ of the anode may be optimized in this configuration to the extent that virtually the entire beam energy is dissipated in the working medium (notice that the electron may experience several aperture oscillations [12]). The number of photoelectrons emitted as a result of deceleration in the DS of a fast electron with the energy w may be represented as $n_{eph} = \mu\eta_{ex} w\gamma_{ph} R/h\nu$,

P A Bokhan Rzhanov Institute of Semiconductor Physics, Siberian Branch of the Russian Academy of Sciences, prosp. Akademika Lavrent'eva 13, 630090 Novosibirsk, Russian Federation
E-mail: bokhan@isp.nsc.ru

Received 31 October 2017, revised 20 April 2018
Uspekhi Fizicheskikh Nauk **188** (12) 1361 – 1366 (2018)
DOI: https://doi.org/10.3367/UFNr.2018.04.038362
Translated by M Zh Shmatikov; edited by A Radzig

where η_{ex} is the fraction of the EB energy contributed to excite the resonance states, γ_{ph} is the photoemission coefficient, $R \sim \mu$ is, in the coaxial configuration of electrodes, the fraction of the vacuum ultraviolet radiation intercepted by the cathode, and $h\nu$ is the quantum energy. For helium, $\eta_{ex} \sim 0.3$ [13], $\gamma_{ph} \approx 0.3$ [14], and $h\nu \approx 22$ eV. At $w = 5$ keV, we get $n_{eph} \approx 20\mu^2$. This means that, beginning with $\mu > 0.25$, the discharge may become the photoelectron discharge. For the conditions $\eta_w \sim \eta_b \sim \mu$ to hold true, a second requirement must be fulfilled: the charge multiplication in the DG must be minimized (η_w is the energy efficiency of EB generation, and η_b is the EB generation efficiency calculated using the formula $\eta_b = I_c/I$, where I_c is the collector current, and I is the discharge current). This requirement may be fulfilled by optimizing the voltage U, p, and pulse duration τ [7]. Therefore, there is nothing enigmatic in implementing the PED and attaining the relation $\eta_w \sim \mu$.

If $\mu \sim 0.9$, i.e., the value that is usually employed in designing laser cells, the conditions of PED being self-sustained are certainly satisfied. It is, therefore, of no importance how large the difference is between η_w and η_b; moreover, if the OD is properly arranged, their values are close to each other [15]. Due to imprisonment of radiation, the arrival of resonance radiation at the cathode is delayed with respect to the event of radiation emission. This delay, which is calculated using the Holstein extraction factor, determines the time during which the current from the cathode sets in (see, for example, the oscillograms shown in Fig. 3 of Ref. [14]); it apparently depends on μ [8, 16]. If the electrodes are arranged in a planar geometry, which is implemented most frequently in studying physical processes, the requirements for the parameters μ and p promoting the OD occurrence become more stringent, primarily due to a reduced value of R. These requirements were specified, for example, in Ref. [17]. The inequality $R > 0.25$ is readily fulfilled in wide-aperture GDs, and the condition for the PED to be self-sustained is easily fulfilled there. The overall understanding of the processes occurring in nanosecond ODs is at the level where simulations reach a predictive power and may be used for determining the conditions under which a particular emission regime prevails [18, 19].

3. Current–voltage characteristics of an anomalous and open discharge

Studies of the current–voltage characteristics (CVCs) of the AD and OD are of importance, since the author of Ref. [9] bases his strongest arguments on studies of the low-pressure AD and extends them to the OD. One can mention as an example frequently quoted papers [20, 21], where the characteristic size of grid holes is $\delta = 1$ mm, and the distance between the electrodes $d = 0.65$ mm. Many authors have studied the CVCs in the AD at higher pressures, which favors the dominant role of photoemission; these studies, while being quite numerous, only spanned the voltage U up to several hundred volts.

To compare the properties of the AD and OD at higher values of U, in preparing this publication we have reproduced the conditions of experiment [20] with different grids: with $\delta = 0.2$; 0.4 ($\mu = 0.88$), and 1 mm as in Ref. [20] for $\mu = 0.92$, and without any grid (AD). Probes for measuring the electric field potential were additionally installed in all cells at a distance of 1.3 and 2 mm from the cathodes. The working diameter of Ti cathodes $D = 12$ mm, and the DS length is 20 mm. Experiments have been conducted both with helium of 99.999% purity and with small admixtures (10–100 mTorr) of O_2 and N_2. To determine the efficiency of EB generation, the energy contributions have been measured in both the DS and an EC. To this end, thermal sensors and heating elements, which were intended for calibration, were installed on the EC and side walls. Studies have been carried out applying various regimes of power supply: continuous current, main voltage half-periods, and rectangular pulses, the duration of which varied from several dozen microseconds to several milliseconds with a ~ 10-μs front. Schematics of the experiment layout and measuring circuit are similar to those displayed in Fig. 1 of Ref. [9]. Two regimes were used to switch on the cells: (a) the anode and EC were grounded via current-measuring shunts, and (b) the EC alone was grounded, and a floating potential was applied to the anode.

The CVC shapes in both the OD and AD proved to be substantially different, dependent on the composition of the mixture, pressure, and power supply regime (Fig. 1). If the helium pressure $p_{He} < 5$ Torr in the AD and $p_{He} < 10$ Torr in the OD, the CVCs are described by smoothly growing curves, the current I in the OD being significantly smaller than in the AD. The current in the AD and OD in pure helium is, in turn, much smaller than in mixtures containing N_2 and O_2. The CVCs correlate in the latter case with those of the Al cathode [22]. For higher pressures ($p_{He} > 40$ Torr), the CVCs for all cells are, quite the opposite, virtually the same and correlate with the CVCs of the normal and weakly anomalous discharges. CVC behavior in the OD for $p_{He} < 30-35$ Torr is much more complex (Fig. 1a, c). Three different regions may be clearly distinguished in the $I(U)$ dependence. The CVCs of all cells in the first region with low U and I are similar to each other. Then, depending on p_{He} and the power supply regime, at some value of I (from 10 to 40 mA), the current no longer depends on U with growing voltage, and the CVC becomes falling in the range $U \sim 0.4-2.0$ kV (region *2*). The smaller δ is, the larger the I decrease in this region (curves *1*, *2*, *3* for $\delta = 0.2$; 0.4; 1 mm, respectively). In the continuous regime, for any value of ballast resistance, as U increases, the low-U discharge rapidly transforms into the high-U discharge, and luminescence appears in the DS. Oscillograms of the current and voltage, if power is supplied in half-periods of main voltage, are displayed in the inset to Fig. 1a. It can be seen that the low-voltage discharge ignites first. Next, a rapid decrease in the current and increase in the voltage consequently occur (over a time of ~ 15 μs), which are followed by glowing at the high-voltage stage and, finally, a transition to the low-voltage stage occurs within a timeframe of 150–200 μs. The CVC for this transition 'stitches' dependence *1* in Fig. 1a ($p_{He} = 30$ Torr, $\delta = 0.2$ mm) in the region of the current–voltage (CV) jump in the range $U = 0.4-1.5$ kV. At the high-voltage stage (region *3*), as U increases, current I increases as well, first slowly and then faster. If power is supplied using $\tau = 1.5$-ms rectangular pulses, the current no longer depends on U in a range from $I = 4$ mA to ~ 50 mA, and afterward U slowly increases (segment *1a* in curve *1*).

The CVC surge for the $\delta = 0.4$-mm cell is smaller than for the $\delta = 0.2$-mm cell (the growth factor reaches 18 and 37, respectively), and the entire curve is shifted to larger currents (curves *2*, *2a*). Virtually no CV jump is observed for the $\delta = 1$-mm cell (dependence *3*). It should be noted that the CV jumps were discovered earlier in nanosecond ODs occurring in He, Ne, and Ar [17]. If the anode is disconnected, i.e., the floating potential regime is applied, the Z-shaped form of the

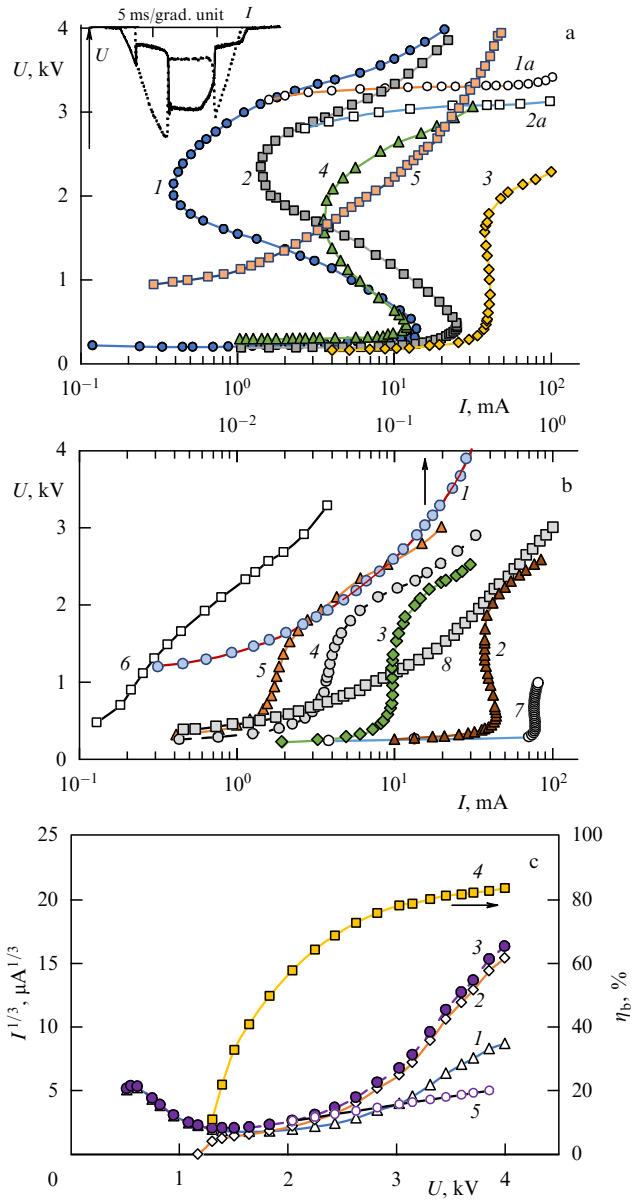

Figure 1. CVC in 'open' and anomalous discharges. (a) OD: curves *1–4* — $p_{He} = 30$ Torr, curve *5* — $p_{He} = 4$ Torr, $p_{O_2} = 60$ mTorr, *1–3* and *5* — grounded anode, *4* — anode under the floating potential. $\delta = 0.2$ mm (*1*, *4*); $\delta = 0.4$ mm (*2*); $\delta = 1$ mm (*3*). Continuous current (*1–4*); rectangular pulse, $\tau = 1.5$ ms (*1a*, *2a*, and *5*). Oscillograms in the inset: $p_{He} = 30$ Torr, $\delta = 0.2$ mm, grounded anode, main voltage half-period. (b) Curve *1* — OD, $\delta = 1$ mm, grounded anode, $p_{He} = 1.5$ Torr, $p_{O_2} = 100$ mTorr. Curves *2–8* — AD at $p_{He} = 28$, 12.5, 8, 6, 1.45, and 4 Torr, respectively, $p_{O_2} = 23$ mTorr, $D = 12$ mm (*2–6*, *8*); $D = 195$ mm (*7*) [23]. (c) OD, $p_{He} = 20$ Torr, $\delta = 0.2$ mm: *1* — anode current, *2* — collector current, *3* — total current, *4* — $\eta_b = I_c/I$, and *5* — dependence $I \sim U^3$.

CVC curve becomes less steep (curve *4* in Fig. 1a, $\delta = 0.2$ mm, $p_{He} = 30$ Torr). This version of power supply to the cell is distinguished by the voltage drop on the cell being larger in the low-voltage stage than in the case of a grounded anode. This phenomenon is explained by the emergence of a difference in potentials between the anode and EC (~ 100 V at the low-voltage, and ~ 150 V at the high-voltage stages), which is needed for maintaining the continuity of the current flow in the discharge circuit. This potential decreases to a value of several volts in the vicinity of the probe located at a distance of 2 mm from the cathode (1.3 mm from the anode).

If the CVC is described by function $I \sim p^x U^y$, then in the range $U = 2.5-3$ kV for the $\delta = 0.2$-mm cell and $p_{He} = 30$ Torr, $y = 10$ for the floating-anode potential, and $y = 15$ for the grounded anode. If power is supplied using rectangular pulses, y stabilizes at $y = 15$ for the floating-potential version, and $y > 50$ for the grounded anode and $I = 3-50$ mA. The parameter y is negative in the range $U \approx 0.4-2$ kV and reaches the value of $y = -5$. Parameter x varies depending on the conditions within the range $x = 1.5-7$ and, in contrast to parameter y, is always positive.

With p_{He} decreasing, all CVCs shift to smaller currents, and their Z-shaped behavior becomes less pronounced. If $p_{He} = 20$ Torr, the entire CVC may be obtained in the continuous power supply regime. Figure 1c shows the OD characteristics for that case. One can see that the EB emerges in the upper part of the Z-shaped characteristic, and the fraction of the current measured by the EC at $U = 4$ kV is $\sim 84\%$ for the grid transparency $\mu = 87\%$; this is an indication of a small charge multiplication rate in the DG. The parameter $y = 10$ in the region $U \sim 3-3.8$ keV, a value that is smaller than that for $p_{He} = 30$ Torr. Curve *5* shows for comparison how the total current varies in the range $U = 2-3.8$ for $y = 3$, as in Eqn (7) in Ref. [9]. The parameter x decreases in the range $U \sim 2-3.8$ kV from $x = 5.85$ to $x = 2.8$. Due to this, if p_{He} decreases further, the current rapidly diminishes, and the Z-shaped CVC vanishes for $p_{He} < 10$ Torr. If $p_{He} < 4$ Torr, the GD is not ignited in any cell for any voltage U up to $U = 6$ kV, the maximum electric strength of the insulating layers between the cathode and anode. Introducing molecular admixtures completely restructures the CVC. The CVC (curve *5*) is shown as an example in Fig. 1a, which corresponds to $\delta = 1$-mm cell in an He–O_2 mixture at $p_{He} = 4$ Torr and oxygen $p_{O_2} = 60$ mTorr, $\tau = 1.5$ ms. If $p_{He} = 1.5$ Torr, as in experiment [20], the CVC for the GD with an admixture of O_2 ($p_{O_2} = 100$ mTorr) in a $\delta = 1$-mm cell is shown in Fig. 1b (curve *1*). It can be seen that $I = 300$ μA for $U = 4$ kV. Given these data, it is not possible to imagine how the current density of ~ 400 mA cm^{-2} was obtained in Ref. [20] (see also Fig. 1*d* there) at $U = 3.6$ kV in helium in a $\delta = 1$-mm cell, and how compliance with the model is realized [21].

The quoted results show that the OD CVC has nothing in common with either the anomalous discharge CVC described by Eqn (7) in Ref. [9] or the results of studies [20, 21]. Therefore, the known properties of the AD may not be automatically extended to the OD. We consider next the AD CVC under increased pressure and voltage (Fig. 1b). Similarly to the OD CVC, one can distinguish three regions in the pressure range $p_{He} = 6-28$ Torr. The AD CVC is similar as a whole to the CVC for the $\delta = 1$-mm cell, as follows from a comparison of dependences *3* in Fig. 1a and *2* in Fig. 1b. Therefore, the design of cells with $\delta \geqslant d$, which were used in Ref. [20], is not adequate for igniting the OD. It should be noted that the negative y value was discovered earlier in the wide-aperture AD with the $D = 19.5$-cm cathode under voltage $U < 1$ kV and $p_{He} = 1.45$ Torr (see Ref. [23], curve *7* in Fig. 1b). Similarly to the OD, the AD in pure He cannot be described by dependence *7* in Ref. [9]. For example, the parameter x in the $U \approx 1-3$-kV range may be as large as $x \approx 5$ and $y \approx 6$ in the $U = 2.2-2.4$-kV range for $p_{He} = 12.5$ Torr. If molecular admixtures are introduced, the CVCs drastically change (compare curves *6* in Fig. 1b ($p_{He} = 4$ Torr) and *8* ($p_{He} = 4$ Torr in the presence of admixed

oxygen with $p_{O_2} = 23$ mTorr) and become similar, but still not identical to the dependences presented in Ref. [9].

4. Efficiency of electron beam generation in an open and anomalous discharge

Figure 2a depicts the U-dependence of η_w, η_b, and the fraction Δ_c of the EB power scattered on the EC for a $\delta = 0.2$-mm cell and $p_{He} = 26$ Torr. One can see that at $U \approx 4$ kV the efficiencies η_w and η_b are close to each other and virtually equal to μ. If $U < 4$ kV, the mismatch increases as U decreases, a behavior that may be explained by the deterioration of conditions for the electron runaway regime and, correspondingly, enhanced multiplication in the DG. The energy lost by the fast electron in the DS weakly depends on U and is $w_e \approx 2$ keV, (Fig. 2b, curve *1*). For the considered version of the cell with $R = 0.17$, yielding the value of $n_{eph} = 4.4\eta_{ex} > 1$ at $U = 4.35$ kV, so that the photoemission discharge is self-sustained. The values of w_e and η_w are significantly smaller in the version with the floating-anode potential (Fig. 2a, curves *1* and *3*). As was noted above, due to the potential jump in front of the anode, ions drift from the DS to DG, as a result of which the fraction of the current transported by the EB diminishes.

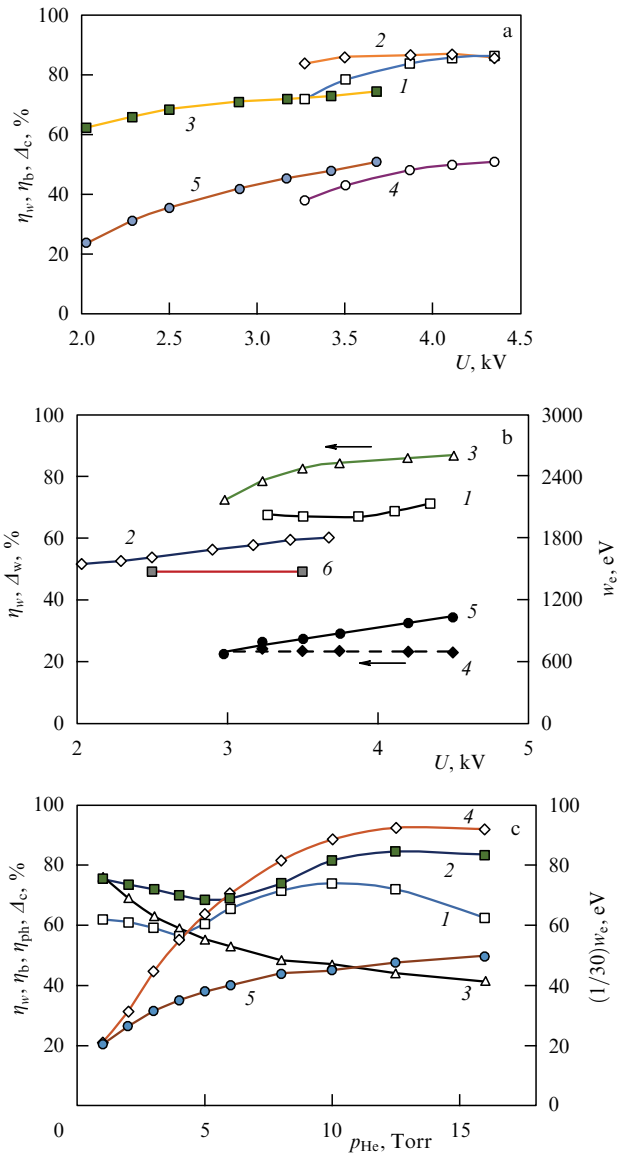

Figure 2. Efficiency of EB generation and the energy deposited to the DS and dissipated in the EC. (a) Efficiency of EB generation in the OD with a grounded anode (*1*, *2*) and floating potential (*3*): η_w (*1*, *3*); η_b (*2*); p_{He} = 26 Torr (*1*, *2*, *4*); p_{He} = 20 Torr (*3*, *5*). The fraction of the power dissipated by EC (*4*, *5*) with the grounded anode and floating potential, respectively. (b) Energy lost by an individual electron in the DS: OD with the grounded anode (*1*), $p_{He} = 26$ Torr, $\delta = 0.2$ mm; OD with the floating anode potential (*2*) $p_{He} = 20$ Torr, $\delta = 0.2$ mm; AD in O_2, $p_{O_2} = 120$ mTorr (*5*); AD in He, $p_{He} = 12.5$ Torr (*6*), Δ_w (*4*) — fraction of the EB power in the GD in O_2 dissipated on the cell wall. Efficiency of EB generation in the GD in O_2 (*3*) at $p_{O_2} = 120$ mTorr. (c) Efficiency η_w in the AD: $U = 2.5$ kV (*1*); $U = 3.5$ kV (*2*); fraction of the EB power (*3*) dissipated on the EC ; fraction of photocurrent (*4*); energy lost by an individual electron in the DS (*5*); curves *1*, *3*, and *5* — continuous discharge, $U = 2.5$ kV; curves *2* and *4* — rectangular pulse, $\tau = 1.5$ ms.

Figure 2c shows how the similar AD characteristics at $U = 2.5$ kV (continuous regime) and $U = 3.5$ kV (power supply with $\tau = 1.5$-ms rectangular pulses) depend on p_{He}. For $p_{He} > 4$ Torr, the measurements have been made in pure He, while for $p_{He} < 4$ Torr an $He-O_2$ mixture with $p_{O_2} = 15$ mTorr was used due to a small amperage of the currents. Comparing curves *1* and *2* in Fig. 2c, one can see the transition from the regime dominated by the emission under the effect of heavy particles ($p_{He} < 4$ Torr) to the regime dominated by photoemission, as pressure and, correspondingly, the photocurrent fraction in the total discharge current increase (curve *4*). However, the same efficiency as in the OD is not gained, since the ion drift in the AD from the DS to the cathode is in no way restricted. It is important to note that the OD with the floating-anode potential represents the case where the CVC and the values of w_e and efficiency are intermediate between those of the AD and the OD with the grounded cathode. This is explained by decreasing the fraction of the current transported by ions as the transition from the AD to the OD with the grounded cathode occurs. The difference between the CVCs in the continuous and quasicontinuous regimes may also be explained, as proceeding due to strong gas heating owing to a large power dissipated in the DS. In the pulse (quasicontinuous) regime, the gas, despite heating, does not have enough time to expand to the buffer zones. Therefore, at least for $\tau = 1.5$ ms and I up to 50 mA, the conditions for the additional photoillumination remain unchanged, and the current does not depend on voltage (Fig. 1a, curves *1a* and *2a*).

5. Emission coefficients in a gas discharge in pure noble gases and their mixtures with molecular gases

Despite numerous studies that have been conducted for many years, the emission coefficients under the effect of fast, $w = 50-1000$ eV, of atoms (γ_a), ions (γ_i), and photons (γ_{ph}) in the GD remain a matter for discussion. The general opinion is that the coefficients γ should be considered in simulations as unknown values [24] to be found as fitting parameters from the solution to the inverse problem using measurements of the actual characteristics of the discharge. The $\gamma_{i,a}$ values for He are often taken in the first approximation from study [26]. A distinguishing feature of this study is that its authors worked for a long time with N_2 and N_2^+ beams with the energy of up to 1 keV [27]. Moreover, the He and He^+ beams used in experiments [26] also contained N_2^+ ions. For this reason, the surface layers of the emitting target were heavily doped with nitrogen atoms and molecules.

The difference between the emission properties of metal targets and those of targets with implanted admixtures is that the energy of the electron released in neutralizing admixture ions may be sufficient to overcome the work function. Therefore, the coefficients $\gamma_{i,a}$ for surfaces with implanted atoms (molecules) featuring a high ionization potential [14, 28, 29] are significantly larger than for clean surfaces [30]. The coefficients $\gamma_{i,a}$ are determined by the cross sections of ionization (excitation) of implanted atoms (molecules) by fast heavy particles accelerated in the region of the cathode fall in potential (CFP) and their mean free paths in the cathode material. Therefore, the data from Ref. [26] are not applicable in the case of pure helium. The emission properties of pure O_2, N_2, He, or their combinations may be expected to be the best in mixtures with O_2, since the cross sections of O_2 ionization by fast O_2 molecules are the largest ones [26, 31].

Figure 2b plots dependence $\eta_w(U)$ for an AD in pure O_2 that reaches the maximum value $\eta_w = 86\%$ at $U = 4.5$ keV, which corresponds to the summarized emission under the effect of heavy particles with $\langle\gamma\rangle \sim 6$. For nitrogen, one has $\eta_w < 80\%$. In $He-O_2$ mixtures with a small content of O_2, both the photoemission mechanism dominating under increased p_{He} and emission under the effect of heavy particles that prevails under low pressure are operative. Therefore, the η_w dependence exhibits an extremal behavior with the minimum in the region close to $p_{He} \approx 4-5$ Torr (Fig. 2c).

The cross section of helium ionization by fast helium atoms [32] is significantly smaller than the N_2 ionization cross section. Therefore, excitation of resonance states followed by the release of electrons in the Auger process becomes the main mechanism of emission from helium-doped targets. The upper limit for the values of $\gamma_{i,a}$ that follows from this mechanism has been found in Ref. [14]. These values are close to their counterparts for the AD in pure He, provided that agreement is attained between the theoretical and experimental results [33]. To describe the left branch of the Paschen curve for $U > 10$ kV, the authors of Ref. [32] had to use even lower values of γ_a. For comparison, if $w = 1$ keV, $\gamma_a = 0.05$ in Ref. [32], while $\gamma_a = 0.2$ in Ref. [33], and $\gamma_a = 1.2$ in Ref. [26]. The mismatch between the results reported in Refs [32, 33] is due to the fact that the former takes into account photoemission, which yields 25% of the current from the cathode for E/N values close to those put on in Ref. [33].

6. Comments and inferences

Utilizing the results presented here and studies of nanosecond ODs, we complete the physical picture of the OD we developed earlier that is in disagreement with the conclusions of [9].

I. *Conditions for feasibility of the open PED and highly efficient generation of the electron beam*. As follows from the curves shown in Fig. 1a, the discharge in the grounded cathode version, for which the highest values $\eta_w \sim \mu$ have been obtained, ignites at $U = 210-215$ V and $pd = 1.95$ Torr cm, i.e., values corresponding to the onset of the left branch of the Paschen curve [34]. As U grows, I grows as well, reaching a maximum at $U = 450-500$ V. This maximum, which is observed at $E/N \approx 7.5\times10^{-15}$ V cm^2, corresponds to the maximum of α, the Townsend multiplication factor [15]. Therefore, a further increase in U results in a decrease in current: the smaller δ is, the bigger the decrease. An explanation for this phenomenon is that for larger δ the field 'extends' to the area behind the anode, thus facilitating an additional injection of ions from the DS into the discharge gap. If $U > 2$ kV, a significant outflow of energy from the DG to the DS occurs (Fig. 1c), and I increases again as a result of EB formation and enhanced additional photoillumination from the DS. If $U > 3.2$ kV, the energy dissipated in the DS is sufficient for generating the number of photons that makes the PED self-sustained.

To obtain a large value of $\eta_w \sim \mu$, a second condition must be fulfilled: the ion current to the cathode must be reduced to a minimum. This may be attained by reducing α owing to an increase in E/N and reduction in δ, which prevents the ions from pulling out of the DS. The reduction in η_w in transition from the grounded-anode OD to the anode-floating-potential OD and next to the AD is explained by the injection (drift) of ions from the DS. Remarkably, photoemission may also prevail in the AD. However, due to a lower energy of the fast electron deposited to the DS (Fig. 2b, c), the condition for the photodischarge in the AD to be self-sustained is not fulfilled. An additional reason for the ion current to be limited in the nanosecond GD is the inertia of heavy particles [15]. As a result of the condition for PED self-sustainability being fulfilled, the current rapidly grows for $U > 3.2$ kV, until the discharge is stabilized as a result of the gas being heated and forced out of the cell volume. This regime is manifested in the most pronounced way if power is supplied in millisecond pulses (Fig. 1a). The discharge development time, which is about 150 μs under these conditions, is driven by the onset of recombination processes enhancing the additional photoillumination [23].

II. *Regarding the arguments allegedly evidencing that the photoelectron discharge is a fiction*. Arguments of this kind may be conventionally divided into two groups. The first includes conclusions based on studies by the author of Ref. [9]. As was shown above, his results are obtained under conditions that are only seemingly similar to the conditions for PED realization: (a) the condition $\delta \ll d$, under which there is no significant cathode erosion [15], is not fulfilled in the majority of cases; (b) the author's experiments were being conducted with working gases, the purity of which is not known, and, arguably, insufficiently 'trained' cells, the results of which are significant differences in the CVCs. There is therefore neither a subject for discussion nor grounds for taking into account the experimental results obtained by the author.

The second group of arguments is based on interpreting the results obtained by other authors. Due to the limited size of this publication, we discuss briefly only some issues that are, in our opinion, of special importance.

(1) The arguments of the author of Ref. [9] are based on referencing the results of studies where either EB generation at $p_{He} \sim 1$ Torr and $U < 10$ kV or features of industrial EBs for $U > 100$ kV and $p_{Ar} \sim 1$ Pa were explored. For obvious reasons, these results may not be applied to the OD, as was stressed as early as in Ref. [35].

(2) In presenting the oscillograms shown in Fig. 2 of Ref. [36], the author of Ref. [9] asserts that those oscillograms are 'typical'. Actually, none of the publications on OD studies contains oscillograms of that kind, where the EB current would appear earlier than the anode current. It was emphasized as early as in publication [6] that the anode current oscillogram always repeats the shape of the collector current. Therefore, one may conclude without a doubt that the oscillogram in Fig. 2, taken from Ref. [36], wherein the EB current is ahead of the anode current, is the 'unique' one

and, most likely, an error. As to the current falling with decreasing U, the author of Ref. [9] overlooks three mechanisms that enhance the additional photoillumination as U increases: (a) the excitation of He resonance states by fast He atoms that drives the development of the discharge for $E/N > 4 \times 10^{-14}$ V cm^2 [17]; (b) the emergence and development of induction and compensation currents [37], which are of special importance at the leading edge of the pulse, and (c) the reflection of electrons from the EC. The last phenomenon is, at low working pressures, virtually the single mechanism responsible for plasma glow in the DS ([38], Fig. 1a). Under our experimental conditions, this process eventually results in the release of $\sim 23\%$ of energy on the wall (curve *4* in Fig. 2b) and an increase in the total power dissipated in the DS for $U > 3.8$ kV (Fig. 2b, curve *1*), while maintaining the self-sustainability of the PED.

(3) The calculated efficiency of the EB generation in He, displayed in Fig. 3 of Ref. [9], may not be extended to the $He-O_2$ mixture in Ref. [38]. Moreover, the result of Ref. [38] is 'unique' at one point, since it is reproduced nowhere else. For example, in the later and extended study [22] by the same authors, the efficiency η_w at $U = 2.4$ kV varies from 0.3 to 0.55 and never reaches the value of $\eta_w = 0.7$. The calculation itself of $\langle\gamma\rangle$ in He is incorrect, since it does not take into account deceleration of fast He atoms by the atoms of the working medium [39]. Should this factor be taken into account, the value of $\langle\gamma\rangle$ diminishes by a factor of two to four [35, 40]. Using more realistic values of $\gamma_{i,a}$ in a self-consistent model of the helium discharge that also agrees with the experiment yields $\langle\gamma\rangle = 0.98$ at $U = 4$ kV [33], in contrast to $\langle\gamma\rangle \approx 5$ displayed in Fig. 3 of Ref. [9]. If photoemission is taken into account [32] for the same values of E/N as in Refs [9, 33], then one obtains $\langle\gamma\rangle = 0.75$.

(4) The photon flux to the cathode and, correspondingly, the photoemission contribution to the discharge current [21, 41] have been calculated with an error exceeding many orders of magnitude due to misunderstanding of the physical meaning of the term 'escape coefficient'. This coefficient defines not an attenuation of the resonance radiation leaving the plasma volume, as assumed by the authors of Refs [21, 41], but an increase in the radiation emission time compared to the lifetime of the atom in the corresponding state (see Fig. 3 in Ref. [14]). The author of Ref. [9] actually 'bans' from functioning, in addition to PED, such devices as luminescence and sodium lamps, plasma displays, and so forth.

(5) The author of Ref. [9] asserts that electrons decelerated in the DS cannot reach the collector. In fact, these electrons drift to the EC under the effect of the EB volume charge and conductively close in this way the discharge current circuit to the EB. To this end, it is sufficient to maintain the collector potential a bit lower than the anode potential. The current in the GD is transported in a similar way from the negative glow region via the dark space to the positive column.

(6) The fact that the ignition voltage in He at $pd = 0.2$ Torr cm is over 100 kV [32], as is the case in Refs [21, 41], is ignored. This gives evidence that the working medium is heavily contaminated [21, 41], and the models constructed do not correspond to actual conditions.

III. *The author of Ref.* [9] *seems to be unaware of many studies that have discovered the discharge phases and types where photoemission dominates*. We only list some of them: (a) initial GD phases in all noble and some molecular gases (see, for example, Refs [42–45]); (b) high-frequency GDs [46–48]; (c) large-volume GDs [48, 49]; (d) GDs with a relatively low value of E/N [34], etc. Some other studies have also been ignored; see, for example, Refs [50, 51], where the value of $\eta_w \approx 1$ was obtained in the OD. The photoemission is also of importance even in nanosecond discharges at $p_{He} \approx 1$ atm and $U \approx 1$ kV, where obviously there is no electron runaway and, hence, no energy outflow from the CFP region.

7. Conclusion

The set of results obtained earlier by many authors, which are quoted above, provides proof that the PED is a phenomenon that has been known for a long time. The distinction between our studies and those made by other authors is that the known discharge types and phases with dominating photoemission, have been distinguished, explored, and optimized for highly efficient EB generation. As to the arguments set forth by the author of Ref. [9], they are based either on using the results of experiments obviously inapplicable to the OD (low-pressure discharges) or on experiments performed by that author under uncontrollable conditions in cells unsuitable for realizing the OD or interpreting, in an arbitrary way, the theoretical and experimental results obtained by other authors and, therefore, do not withstand criticism. It should be emphasized that reproducible results in exploring the OD may only be obtained in clean experimental conditions.

References

1. Bokhan P A, Sorokin A R *Sov. Phys. Tech. Phys.* **30** 50 (1985); *Zh. Tekh. Fiz.* **55** 88 (1985)
2. Dreicer H *Phys. Rev.* **115** 238 (1959)
3. Babich L P *High-Energy Phenomena in Electric Discharges in Dense Gases: Theory, Experiment, and Natural Phenomena* (Arlington, Va: Futurepast, 2003)
4. Bokhan P A, Kolbychev G V *Sov. Phys. Tech. Phys. Lett.* **6** 180 (1980); *Pis'ma Zh. Tekh. Fiz.* **6** 418 (1980)
5. Bokhan P A, Kolbychev G V *Sov. Phys. Tech. Phys.* **26** 1057 (1981); *Zh. Tekh. Fiz.* **51** 1823 (1981)
6. Kolbychev G V, Samyshkin E A *Sov. Phys. Tech. Phys.* **26** 1185 (1981); *Zh. Tekh. Fiz.* **51** 2032 (1981)
7. Kolbychev G V, PhD Thesis (Phys.-Math. Sci.) (Tomsk, 1983)
8. Kolbychev G V, Ptashnik I V *Sov. Phys. Tech. Phys. Lett.* **11** 458 (1985); *Pis'ma Zh. Tekh. Fiz.* **11** 1106 (1985)
9. Sorokin A R *Phys. Usp.* **61** 1234 (2018); *Usp. Fiz. Nauk* **188** 1354 (2018)
10. Sorokin A R *Tech. Phys. Lett.* **21** 832 (1995); *Pis'ma Zh. Tekh. Fiz.* **21** (20) 37 (1995)
11. Bokhan P A, in *Entsiklopediya Nizkotemperaturnoi Plazmy* (Encyclopedia of Low-Temperature Plasma) Vol. XI-4 (Ed. S I Yakovlenko) (Moscow: Fizmatlit, 2005) p. 322
12. Bokhan P A, Zakrevsky Dm E, Gugin P P *Phys. Plasmas* **18** 103112 (2011)
13. Syts'ko Yu I, Yakovlenko S I *Sov. J. Plasma Phys.* **2** 34 (1976); *Fiz. Plazmy* **2** 63 (1976)
14. Bokhan P A, Zakrevsky D E *Tech. Phys.* **52** 104 (2007); *Zh. Tekh. Fiz.* **77** 109 (2007)
15. Bokhan A P, Bokhan P A, Zakrevsky D É *Plasma Phys. Rep.* **32** 549 (2006); *Fiz. Plazmy* **32** 599 (2006)
16. Kolbychev G V, Ptashnik I V *Sov. Phys. Tech. Phys.* **34** 1018 (1989); *Zh. Tekh. Fiz.* **59** (9) 104 (1989)
17. Bokhan P A et al. *Tech. Phys.* **60** 1472 (2015); *Zh. Tekh. Fiz.* **85** (10) 58 (2015)
18. Schweigert I V et al. *Plasma Sources Sci. Technol.* **90** 044005 (2015)
19. Schweigert I V et al. *Plasma Phys. Rep.* **42** 666 (2016); *Fiz. Plazmy* **42** 658 (2016)
20. Sorokin A R *Tech. Phys. Lett.* **29** 404 (2003); *Pis'ma Zh. Tekh. Fiz.* **29** (10) 15 (2003)
21. Karelin A V *Laser Phys.* **14** 15 (2004)

22. Rocca J J et al. *J. Appl. Phys.* **56** 790 (1984)
23. Belskaya E V, Bokhan P A, Zakrevsky Dm E *Appl. Phys. Lett.* **93** 091503 (2008)
24. Phelps A V *Plasma Sources Sci. Technol.* **10** 329 (2001)
25. Marić D et al. *Eur. Phys. J. D* **21** 73 (2002)
26. Hayden H C, Utterback N G *Phys. Rev.* **135** A1575 (1964)
27. Utterback N G, Miller G H *Phys. Rev.* **124** 1477 (1961)
28. Bokhan P A, Zakrevsky D E *JETP Lett.* **96** 133 (2012); *Pis'ma Zh. Eksp. Teor. Fiz.* **96** 139 (2012)
29. Bokhan P A, Zakrevsky D E *Phys. Rev. E* **88** 013105 (2013)
30. Baragiola R A, in *Low Energy Ion-Surface Interactions* (Ed. J W Rabalais) (Chichester: J. Wiley, 1994) p. 187
31. Utterback N G *Phys. Rev.* **129** 219 (1963)
32. Xu L et al. *Phys. Plasmas* **24** 093511 (2017)
33. Hartmann P et al. *Jpn. J. Appl. Phys.* **42** 3633 (2003)
34. Marić D et al. *Eur. Phys. J. D* **68** 155 (2014)
35. Kolbychev G V *Opt. Atmos. Okeana* **14** 1056 (2001)
36. Kolbychev G V *Opt. Atmos. Okeana* **6** 635 (1993)
37. Kolbychev G V *Izv. Vyssh. Uchebn. Zaved. Fiz.* **42** (11) 84 (1999)
38. Yu Z, Rocca J J, Collins G J *J. Appl. Phys.* **54** 131 (1983)
39. Wilson W D, Haggmark L G, Biersack J P *Phys. Rev. B* **15** 2458 (1977)
40. Ul'yanov K N, Chulkov V V *Sov. Phys. Tech. Phys.* **33** 201 (1988); *Zh. Tekh. Fiz.* **58** 328 (1988)
41. Karelin A V, Sorokin A R *Plasma Phys. Rep.* **31** 519 (2005); *Fiz. Plazmy* **31** 567 (2005)
42. Phelps A V *Phys. Rev.* **117** 619 (1960)
43. Schweigert V A *Teplofiz. Vys. Temp.* **26** 436 (1988)
44. Agache M, Fitaire M, Leduc E *J. Phys. D* **29** 1217 (1996)
45. Ganter R et al. *J. Appl. Phys.* **91** 992 (2002)
46. Baranov I Ya *Plasma Phys. Rep.* **28** 71 (2002); *Fiz. Plazmy* **28** 77 (2002)
47. Baranov I Ya, Koptev A V *Plasma Phys. Rep.* **33** 54 (2007); *Fiz. Plazmy* **33** 56 (2007)
48. Tian P, Kushner M J *Plasma Sources Sci. Technol.* **26** 024005 (2017)
49. Nakamura K, Ando M, Sugai H *Nucl. Instrum. Meth. Phys. Res. B* **206** 798 (2003)
50. Mitko S V et al. *Rev. Sci. Instrum.* **76** 013101 (2005)
51. Mitko S V, Ochkin V N, in *Generatsiya Ubegayushchikh Elektronov i Rentgenovskogo Izlucheniya v Razryadakh Povyshennogo Davleniya* (Generation of Runaway Electrons and X-Ray in the Discharges of High Pressure) (Ed. V F Tarasenko) (Tomsk: STT, 2015) p. 403
52. Fierro A et al. *J. Phys. D* **50** 065202 (2017)
53. Donkó Z, Hamaguchi S, Gans T *Plasma Sources Sci. Technol.* **27** 054001 (2018)